

# Characterization of graphene-covered SiN waveguide using four-wave mixing

Koen Alexander,<sup>1,2</sup> Bart Kuyken,<sup>1,2</sup> and Dries Van Thourhout<sup>1,2</sup>

<sup>1</sup> Photonics Research Group, INTEC, Ghent University-IMEC, Ghent B-9000, Belgium

<sup>2</sup> Center for Nano-and Biophotonics (NB-Photonics), Ghent University, Ghent B-9000, Belgium

*We characterize the nonlinear response of graphene-covered SiN waveguides by means of degenerate four-wave mixing. It is shown that the nonlinear response of graphene is highly dispersive and decreases strongly with increasing detuning between the pump and the signal. The measured magnitude of the nonlinear parameter  $\gamma$  ranges from  $\sim 150 \text{ m}^{-1}\text{W}^{-1}$  to over  $1600 \text{ m}^{-1}\text{W}^{-1}$ , the corresponding nonlinear susceptibility from  $\sim 2 \cdot 10^{-15}$  to  $\sim 2 \cdot 10^{-14} \text{ m}^{-2}\text{V}^{-2}$ .*

## Introduction

Graphene has extraordinary electrical and optical properties, originating from its two-dimensional crystal structure and its linear and gapless band structure [1]. In optics, graphene has been successfully used to make mode-locked fiber lasers [2], by making use of its strong broadband absorption and ultra-fast carrier dynamics. Graphene is also compatible with conventional CMOS technology, which has led to the demonstration of integrated electro-absorption modulators [3]. Both theoretical predictions [4–6] and experimental studies [7–10] have indicated that graphene also has a strong and broadband optical nonlinearity  $\chi^{(3)}$ . However, there seems to be a strong discrepancy between the different reported values. The reasons for this were discussed by Dremetsika et al. in [10]. The nonlinearity of graphene is also expected to be tunable, as multiple theoretical papers have suggested that the dependence of doping level can be remarkably strong [4–6]. In this work, we have integrated the graphene with a SiN waveguide, and we characterize the nonlinearity through four-wave mixing (FWM). FWM experiments have the advantage that they can be done using CW sources. This way difficulties regarding the use of ultrashort pulses are avoided (damage, uncertainties of the exact pulse shape, etc.).

## Device fabrication

A set of straight waveguides (made in a CMOS pilot line) of different widths and lengths was prepared. The SiN structures are initially covered with an oxide layer of  $1 \mu\text{m}$  which was thinned down by means of RIE (Reactive Ion Etching). Figure 1a shows the waveguide cross-section. The thickness of the waveguide is about 330 nm and the residual oxide layer is about 30 nm thick. Subsequently, CVD-grown (Chemical Vapor Deposition) single layer graphene was transferred to the samples at Graphenea [11]. Figure 1b shows the fundamental TE-mode in such a waveguide.

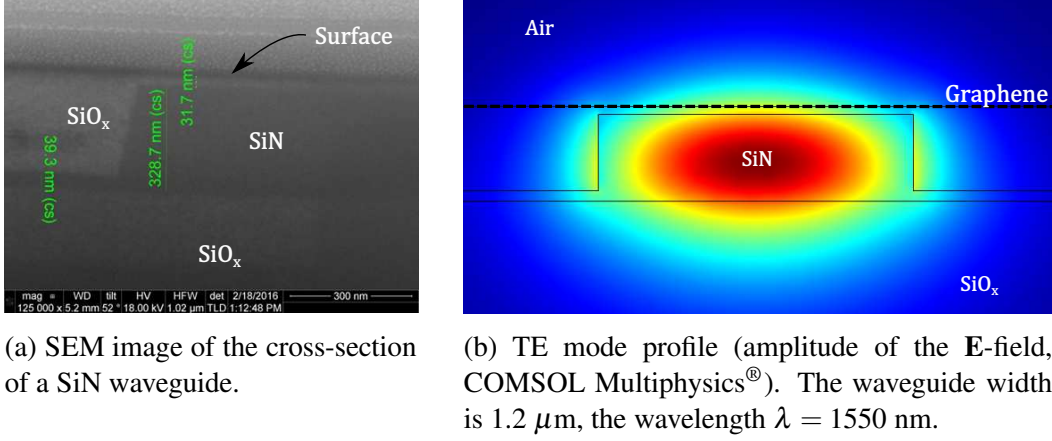


Figure 1: (a) Cross-section of a waveguides and (b) the simulated first order TE mode.

## Four-wave mixing in the SiN/graphene waveguide

**Theory** In a (degenerate) FWM experiment a strong pump (amplitude  $A_{\omega_p}$ , frequency  $\omega_p$ ) and probe signal (amplitude  $A_{\omega_s}$ , frequency  $\omega_s = \omega_p + \Delta\omega$ ) are injected in the waveguide. If the nonlinearity is large enough, an idler wave at frequency  $\omega_i = \omega_p - \Delta\omega$  arises ( $A_{\omega_i}$ ). For the experiments, we can assume that  $|A_{\omega_p}| \gg |A_{\omega_s}| \gg |A_{\omega_i}|$ ,  $A_{\omega_i}(z=0) = 0$  and that the process is always phase matched. The latter is the case due to the short effective interaction lengths. Based on the coupled wave equations one can then prove that:

$$\eta \equiv \frac{P_i(L)}{P_s(L)} = \frac{|A_{\omega_i}|^2}{|A_{\omega_s}|^2} \approx |\gamma_{FWM, \omega_p, \omega_s}|^2 \frac{\omega_i}{\omega_p} |P_p(0)|^2 e^{(\alpha_s - \alpha_i)L} L_{eff}^2 \quad (1)$$

$\eta$  is the nonlinear conversion efficiency,  $L_{eff} \equiv \frac{1 - e^{-(\alpha_p + \frac{\alpha_s}{2} - \frac{\alpha_i}{2})L}}{\alpha_p + \frac{\alpha_s}{2} - \frac{\alpha_i}{2}}$  the effective interaction length,  $\alpha_p$ ,  $\alpha_s$  and  $\alpha_i$  the respective absorption coefficients for pump, signal and idler. By measuring  $\eta$  as a function of signal detuning  $\Delta\omega$  we can calculate the nonlinear coefficient of the waveguide  $|\gamma_{FWM, \omega_p, \omega_s}|$ . From this, the surface third order susceptibility  $|\chi_s^{(3)}(\omega_p, \omega_p, -\omega_s)|$  can be estimated using:

$$\gamma_{FWM, \omega_p, \omega_s} \approx \frac{3\omega_p}{8cn_{eff, i}} \chi_s^{(3)}(\omega_p, \omega_p, -\omega_s) \cdot \frac{\int_G (\mathbf{F}_{\omega_p, \parallel} \cdot \mathbf{F}_{\omega_i, \parallel})(\mathbf{F}_{\omega_p, \parallel} \cdot \mathbf{F}_{\omega_s, \parallel}) dS}{\iint_{-\infty}^{\infty} |\mathbf{F}_{\omega_i}|^2 dx dy} \quad (2)$$

$\mathbf{F}$  refers to the normalized mode profile,  $\int_G$  is a line integral along the graphene surface and the subscript  $\parallel$  refers to the component of the field parallel to the graphene sheet.

**Setup** In figure 2 a sketch of the setup used for the FWM experiment is shown. For the pump, a Syntune S7500 laser with a wavelength around 1550 nm is amplified using

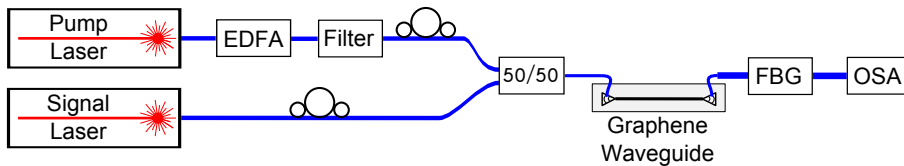


Figure 2: Sketch of the setup used for the four-wave mixing (FWM) experiment.

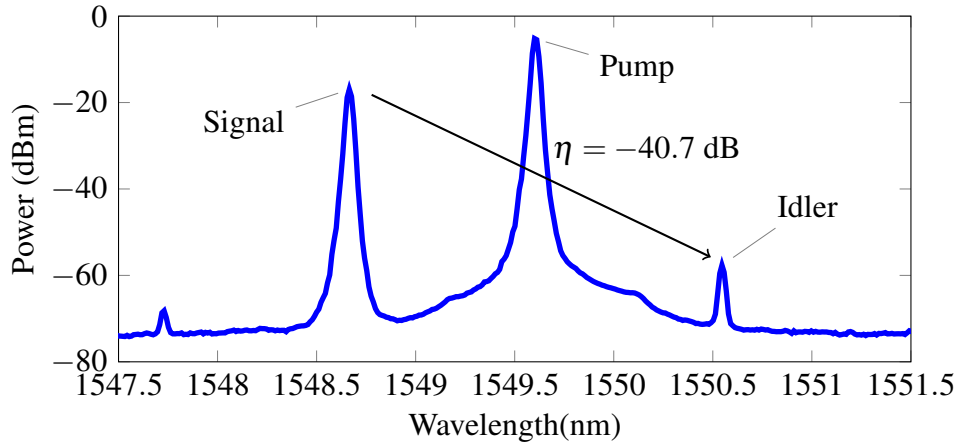
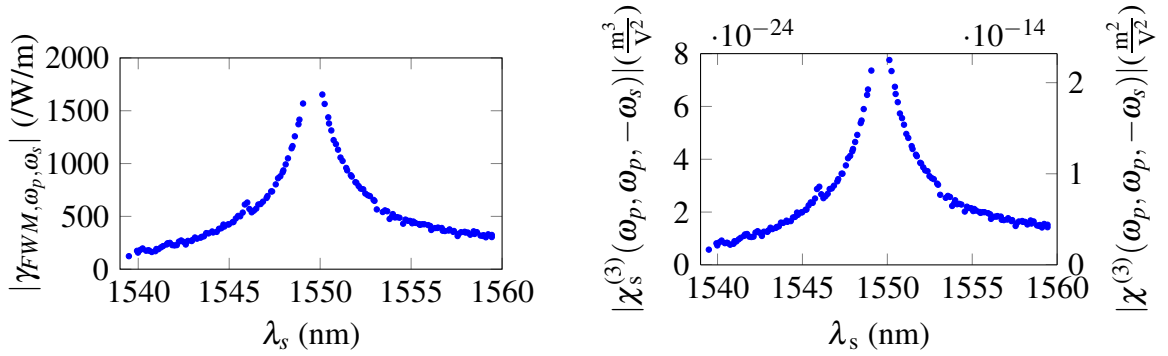


Figure 3: Example of a FWM measurement on a graphene-covered waveguide, output spectrum of the waveguide when injecting the pump and signal ( $L = 500\mu\text{m}$ ).



(a) Estimated nonlinear coefficient of the waveguide as a function of signal wavelength.

(b) Estimated surface and bulk nonlinear susceptibilities as a function of signal wavelength.

Figure 4: (a) The corresponding estimated nonlinear coefficient and (b) the estimated surface and bulk nonlinear susceptibilities. The on-chip pump power was estimated to be  $P_p(0) = 33.5 \text{ mW}$ ,  $L = 500 \mu\text{m}$  and  $\lambda_p = 1549.6 \text{ nm}$ .

an Opto-Link C-band Single Channel 33dBm EDFA. For the signal a Santec Tunable Laser TSL-510 is used. Both lasers are combined and injected into a graphene-covered SiN waveguide. At the end of the waveguide, pump light is being filtered out by a fiber Bragg grating (FBG) and the signal and idler are collected and measured using an Anritsu MS9740A optical spectrum analyser (OSA).

**Experiments and results** Figure 3 shows an example of a FWM measurement, for this measurement the FBG has been removed for illustrative purposes. A strong pump (1549.61 nm) and a weaker signal (1548.67 nm) are injected. A clear peak at the idler wavelength (1550.55 nm) arises. Note that another small peak arises at 1547.73 nm, this due to a FWM process where the roles of the pump and the signal have been switched. Next, the nonlinear parameter was measured as function of the signal detuning, for this the signal wavelength was swept and the conversion efficiency  $\eta$  was measured for each

signal wavelength. This data is then corrected for the wavelength-dependence of the grating couplers and the fiber-optic components and equation (1) was used to estimate  $|\gamma_{FWM, \omega_p, \omega_s}|$ . The result is shown on figure 4a. Using equation (2) the surface nonlinear susceptibility  $\chi_s^{(3)}(\omega_p, \omega_p, -\omega_s)$  can be estimated. The result is plotted in figure 4b. The axis on the left-hand side shows the surface susceptibility, the axis on the right-hand side the effective bulk susceptibility (assuming a monolayer thickness of 0.345 nm).

## Conclusion

From figure 4 it is clear that the nonlinear response of graphene is highly dispersive. When the detuning is small there is strong resonant enhancement and  $\chi^{(3)} > 2 \cdot 10^{-14} \text{ m}^{-2}\text{V}^{-2}$ . For large detunings  $\chi^{(3)}$  drops by more than an order of magnitude, nonetheless the bulk susceptibility remains very large compared to other materials (for Si,  $\chi^{(3)} \approx 3 \cdot 10^{-18} \text{ m}^{-2}\text{V}^{-2}$  [12]). The waveguide nonlinearity ranges from several hundreds to  $\sim 1600 \text{ m}^{-1}\text{W}^{-1}$  close to resonance. This is comparable to the values found for a Si nanowire waveguide. For now, the main drawback of graphene as a nonlinear material is its large linear absorption (roughly two orders of magnitude larger than the state of the art Si and III-V waveguides). It remains to be seen whether gating can mend this problem, by simultaneously decreasing the absorption and increasing the nonlinearity. In the future, we aim to gate the graphene using an ionic gel [13]. This way the dependence of the nonlinear susceptibility and linear absorption on doping level can be probed. This work was partly supported by the Graphene Flagship Project and FWO Flanders.

## References

- [1] F. Bonaccorso, Z. Sun, T. Hasan, and A. Ferrari, "Graphene photonics and optoelectronics," *Nature photonics*, vol. 4, no. 9, pp. 611–622, 2010.
- [2] Q. Bao, H. Zhang, Y. Wang, Z. Ni, Y. Yan, Z. X. Shen, K. P. Loh, and D. Y. Tang, "Atomic-layer graphene as a saturable absorber for ultrafast pulsed lasers," *Advanced Functional Materials*, vol. 19, no. 19, pp. 3077–3083, 2009.
- [3] Y. Hu, M. Pantouvaki, J. Campenhout, S. Brems, I. Asselberghs, C. Huyghebaert, P. Absil, and D. Thourhout, "Broadband 10 gb/s operation of graphene electro-absorption modulator on silicon," *Laser & Photonics Reviews*, 2016.
- [4] J. L. Cheng, N. Vermeulen, and J. E. Sipe, "Numerical study of the optical nonlinearity of doped and gapped graphene: From weak to strong field excitation," *Phys. Rev. B*, vol. 92, p. 235307, Dec 2015.
- [5] B. Semnani, A. H. Majedi, and S. Safavi-Naeini, "Nonlinear quantum optical properties of graphene," *Journal of Optics*, vol. 18, no. 3, p. 035402, 2016.
- [6] S. A. Mikhailov, "Quantum theory of the third-order nonlinear electrodynamic effects of graphene," *Phys. Rev. B*, vol. 93, p. 085403, Feb 2016.
- [7] E. Hendry, P. J. Hale, J. Moger, A. K. Savchenko, and S. A. Mikhailov, "Coherent nonlinear optical response of graphene," *Phys. Rev. Lett.*, vol. 105, p. 097401, Aug 2010.
- [8] H. Zhang, S. Virally, Q. Bao, L. K. Ping, S. Massar, N. Godbout, and P. Kockaert, "Z-scan measurement of the nonlinear refractive index of graphene," *Opt. Lett.*, vol. 37, pp. 1856–1858, Jun 2012.
- [9] L. Miao, Y. Jiang, S. Lu, B. Shi, C. Zhao, H. Zhang, and S. Wen, "Broadband ultrafast nonlinear optical response of few-layers graphene: toward the mid-infrared regime," *Photon. Res.*, vol. 3, pp. 214–219, Oct 2015.
- [10] E. Dremetsika, B. Dlubak, S.-P. Gorza, C. Ciret, M.-B. Martin, S. Hofmann, P. Seneor, D. Dolfi, S. Massar, P. Emplit, and P. Kockaert, "Measuring the nonlinear refractive index of graphene using the optical kerr effect method," *Opt. Lett.*, vol. 41, pp. 3281–3284, Jul 2016.
- [11] "www.graphenea.com," 2016.

- [12] R. W. Boyd, *Nonlinear optics*. Academic press, 2003.
- [13] V. Thareja, J.-H. Kang, H. Yuan, K. M. Milaninia, H. Y. Hwang, Y. Cui, P. G. Kik, and M. L. Brongersma, “Electrically tunable coherent optical absorption in graphene with ion gel,” *Nano letters*, vol. 15, no. 3, pp. 1570–1576, 2015.